Fabrication of Metal-Matrix Composites by Application of the Superplasticity Effect

V.V. Astanin, O.A. Kaibyshev, L.A. Imayeva, and A.A. Sirenko

The production of continuous-fiber metal-matrix composites (MMCs) with improved mechanical properties by solid-state consolidation under superplastic conditions was investigated. The finite-element method was used to model MMC consolidation, which was experimentally studied on a sample of boron-aluminum composite. It was shown that the deformation properties of a matrix exert considerable influence on metal flow geometry and its strain-stress state. The superplasticity effect provides the straightening of a matrix flow front and the localization of an intense deformation zone. It also facilitates the removal of pores in the final stage of hardening and considerably decreases local stresses on the fiber surface. The features of matrix material flow during consolidation of composites were considered. It was shown that the matrix deformation during composite consolidation takes place in the form of cooperative grain-boundary sliding and intragranular sliding. The mechanism of matrix deformation determines a type of fiber-matrix reaction at the interface, or, alternatively, the type of fiber-matrix interface interaction depends on the intensity of localized deformation in the given area. Identification of the interface structure was performed by acoustic emission.

Keywords aluminum alloys, composites, superplasticity

1. Introduction

Continuously reinforced metal-matrix composites (MMCs) with a matrix based on a light metal such as aluminum, magnesium, titanium, or titanium aluminide in combination with boron, silicon carbide, or sapphire fibers from 100 to 200 μm in diameter can be used to fabricate parts that undergo high stresses at elevated temperatures (Ref 1). Application of these composites is attractive for gas turbine engines (GTEs) (Ref 2, 3). The use of high-cost fibers pays for itself by considerably enhancing the technical characteristics of parts. The efficacy of fiber use is determined primarily by the technology of MMC fabrication; in the process of composite consolidation, some reduction in fiber strength, and even fiber fracture, usually takes place, resulting in a 20 to 30% loss of real composite strength (Ref 3, 4). In this regard, the development of composite fabrication technology that provides maximum initial fiber properties is of great importance.

As a rule, a typical process for production of composite parts includes several stages: preparation of a preform from reinforcing fibers, preparation of preforms of matrix material, calculation of required dimensions and cutting of stocks, assembly of semiproducts, consolidation of parts, and quality control of finished artifacts.

Consolidation of composite parts is a major operation. Solid-state consolidation methods offer a number of advantages over liquid-state consolidation because of the elevated chemical activity of melts and increased stresses that occur during cooling from a temperature of solidification. Hot isostatic pressing (HIP) under superplastic (SP) conditions is the most attractive of all solid-state consolidation methods (Ref 5-8). Superplasticity allows processing temperatures and pressures to be decreased and thus reduces damage to the reinforcements. Furthermore, SP deformation favorably affects solid-phase bonding (Ref 9-12), contributing to an improvement of matrix-matrix contact. The processing of a part under SP conditions increases the stress-relaxation capability of many materials, especially brittle ones (Ref 13), which enhances resistance to crack displacement in composites.

This paper investigates the production of composite materials with improved mechanical properties by the solid-state consolidation method under SP conditions. The initial temperature, strain rate, and strain-rate sensitivity coefficient data obtained by tensile tests for the given matrix alloy structure state allow a diffusion bonding regime to be established. Successful pressing of a packet under SP conditions also requires knowledge of the loading law that describes the SP matrix flow during composite consolidation. The pressure should be sufficient for complete filling of the clearances between fibers, but at the same time must be limited to maintain the fibers. Mathematical modeling provides a rational solution.

2. Modeling of MMC Consolidation

This study investigated the consolidation of a unidirectional multilayer foil-fiber-foil composite with square distribution of fibers using the finite-element method (FEM) of metal flow analysis (Ref 14-16). Rheological characteristics for commercial Al-5.8Mg-0.5Mn alloys in normal and superplastic states were used (Ref 16). For mathematical description of the matrix material flow between fibers, a fourth unit cell in the form of rectangle ABCD was examined (Fig. 1). Since fiber length considerably exceeds other cell sizes, only two dimensions are considered. The matrix was divided into triangular elements of different magnitude. Smaller elements were in the areas with expected high gradients of stresses and strains, and larger elements were outside these areas. This provided the required detail under a limited number of computer simulations. The

V.V. Astanin, O.A. Kaibyshev, L.A. Imayeva, and **A.A. Sirenko,** Institute for Metals Superplasticity Problems, Russian Academy of Sciences, Khalturina 39, Ufa, 450001, Russia, vast@ipsm.bashkiria.su.

medium was assumed to be nonlinearly viscous. The stress tensors deviators, S_{ij}, are given by:

$$S_{ij} = 2\mu\xi_{ij} \quad \text{(Eq 1)}$$

where ξ_{ij} is the strain-rate deviator and μ is the viscosity coefficient, which is a function of the strain-rate intensity, $\dot{\varepsilon}_i$, and is experimentally defined by tensile tests:

$$\mu = \mu(\dot{\varepsilon}_i) \quad \text{(Eq 2)}$$

The relation between ball stress tensors and ball strain tensors can be written as:

$$\sigma_0 = k\varepsilon_0 \quad \text{(Eq 3)}$$

where $\sigma_0 = \frac{1}{3}\sigma_{ij}$, $\varepsilon_0 = \frac{1}{3}\varepsilon_{ij}$ are ball stress and strain tensors, respectively, and k is Young's modulus.

Taking into account the results from Ref 17, the basic relationships are limited to the system of linear equations:

$$[\mathbf{K}]\{\delta\} = \{\mathbf{R}\} \quad \text{(Eq 4)}$$

where $[\mathbf{K}]$ is the stiffness matrix, $\{\delta\}$ is the vector of node velocities of a triangular elements mesh, and $\{\mathbf{R}\}$ is the node forces vector.

Since the matrix coefficients $[\mathbf{K}]$ and $\{\mathbf{R}\}$ depend on $\{\delta\}$; the system can be solved by a method of simple iterations. In this paper the calculation was performed at noted instants of time, which corresponded to different MMC consolidation stages, with a step of $\Delta\tau$. After modeling the consolidation process under conditions, a pattern of optimal strain rates was determined. Friction forces exerted proportionally to the normal pressure were taken into account for nodes that were in contact with fiber. A friction coefficient was assumed to be 0.35 (Ref 18).

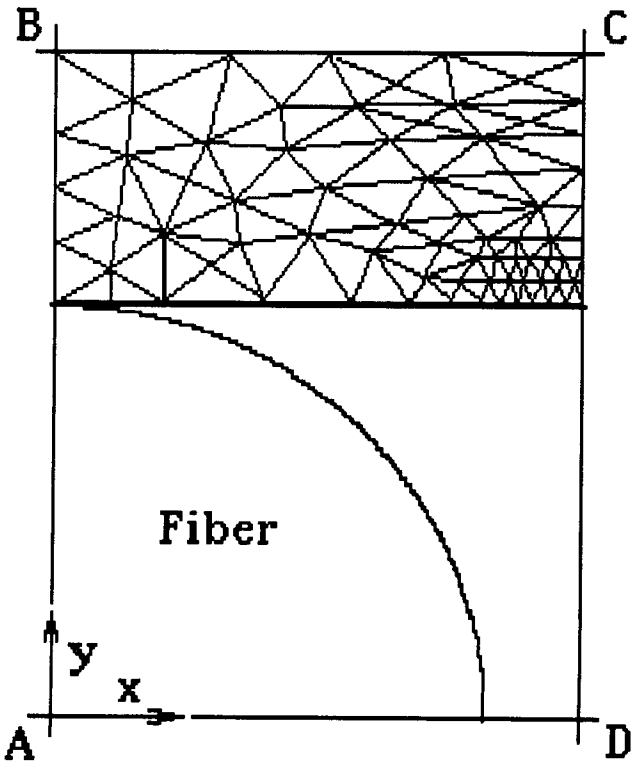

Fig. 1 Unit MMC cell with an initial FEM grid

The FEM (finite element method)-calculated metal flow after MMC consolidation by 12 and 18% at normal and SP conditions is shown in Fig. 2. The effect of rheological properties on the character of a matrix material is readily illustrated by stress contours. In the case of SP deformation, the matrix flow localizes near the fiber surface in the form of an insignificant ridge. The surface ridge affects the flow front, making it straighter. This results in decreased size of pores arranged near the fiber along the x-axis after matrix layers contact in clearances between the fibers. These results fit well with the experimental data obtained previously (Ref 5, 19).

The FEM simulation provides interesting data on the stress distribution at different stages of composite consolidation. In the initial stage (Fig. 2a, c), the most intensive stresses operate in a layer that is 30 to 40% of the foil thickness, t, its lower boundary being at a distance of $(0.1...0.15)t$ from the fiber surface. As the composite is consolidated, the intensive stress zone moves along the fiber surface, and in the final stage of the process it transfers to the ridge point where adjacent matrix layers are joined together. The same is observed in zones of intensive deformation since intensities of stress and strain rate are connected with each other. These features are important for understanding interaction processes at fiber-matrix and matrix-matrix interfaces.

Two typical distinctions in the behavior of normal and SP materials should be noted. The first distinction involves localization of the zone of the maximum intensity of stresses, σ_i. During SP deformation the width of the zone along the fiber surface is less than half of that found during normal processing. In other words, SP material flow compared to usual flow is more localized in the deformation front that aligns close to the fiber surface (stress line 2 in Fig. 2d). The second distinction concerns extreme contact stresses that affect the fiber. The peak contact stress occurs at 6% consolidation of the composite—that is, at the initial stage of consolidation. It is localized in the pole part of the fiber and reaches 22 MPa in the case of SP deformation and runs to 150 MPa in the case of normal plastic deformation. As this takes place, the strain forces defined by integration of σ_y with respect to line BC (Fig. 1) constitute 8 and 14 MPa, respectively. The positive effect of the matrix superplasticity is apparent here since a high value of the localized stress leads to degradation or failure of the fibers.

By integrating σ_y with respect to line BC, the load providing the matrix deformation under SP conditions at all degrees of consolidation (ε) was defined (Fig. 3). Experimental data obtained during hot pressing of composite specimens with a matrix of commercial Al-5.8Mg-0.5Mn alloy also are shown. Comparison of the curves reveals their mutual consistency. Together with structural investigation, this confirms that the model describes rather exactly the MMC consolidation process.

3. Experimental Method

3.1 *Preform Preparation*

Boron fiber woven nets were used to fabricate the composite. The boron fibers were 140 μm in diameter, with an average strength of 2900 MPa and a fiber tensile strength distribution variation coefficient of 15%. The nets were manufactured using a standard metal loom that was modified for processing high-modulus brittle fibers. The textile method allowed reliable location of the fibers at a given distance from one another as well as qualitative cutting and stacking of complex-shape stocks. A fine wire of pure aluminum was used to locate the fibers (Fig. 4). The wire diameter was within a range of 20 to 50 μm; the spacing between the wires was within 3 to 5 mm. In this case the volume content of wire in the composite does not exceed several percent and does not significantly affect composite properties. The fiber stacking step, depends on the fiber

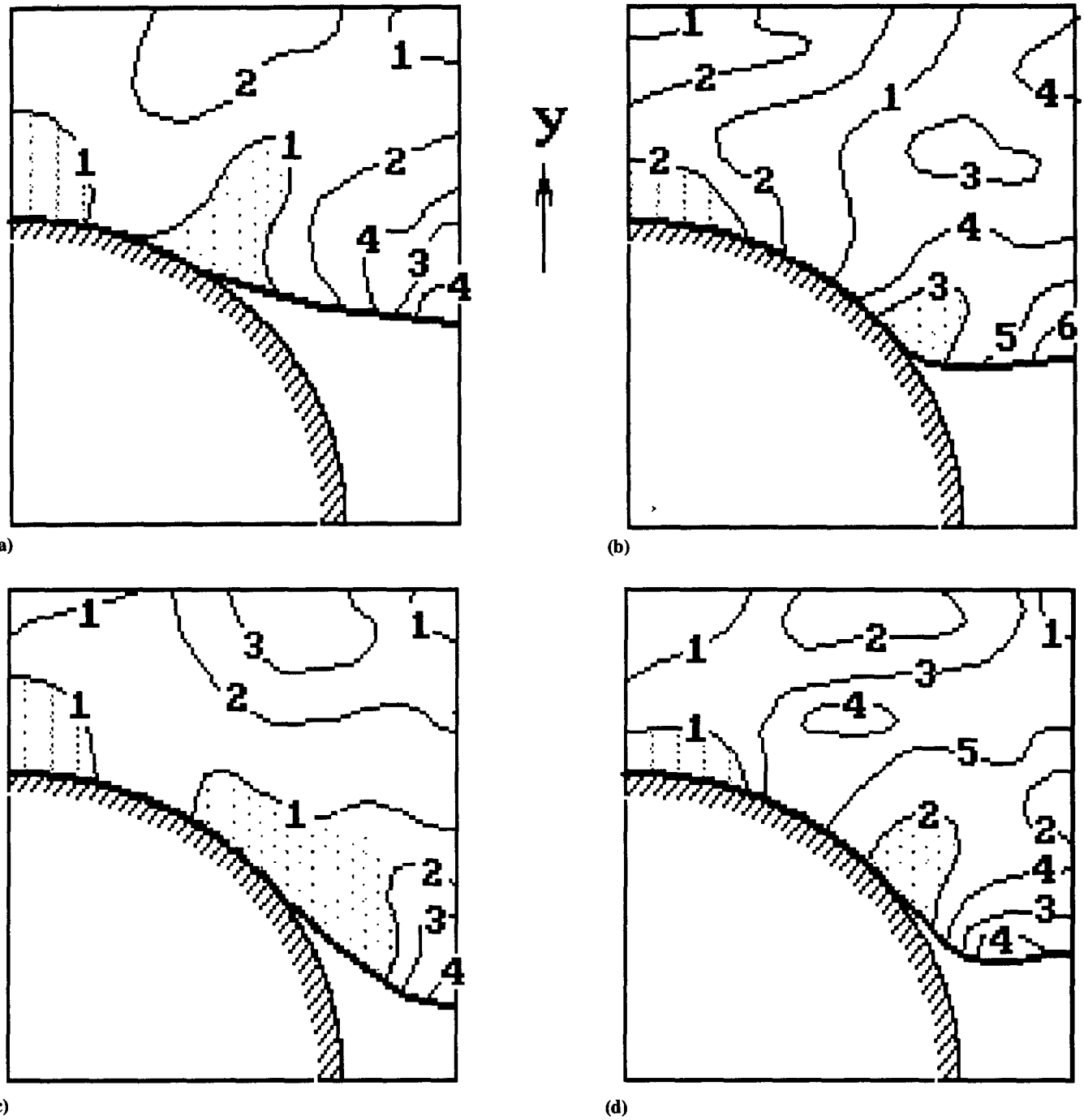

Fig. 2 FEM-predicted metal flow after normal (a, b) and superplastic (c, d) deformation by 12% (a, c) and 18% (b, d). Each figure corresponds to a definite stress intensity (MPa): (a) 1 = 152, 2 = 110, 3 = 79, 4 = 57; (b) 1 = 146, 2 = 132, 3 = 139, 4 = 119; (c) 1 = 15, 2 = 17.5, 3 = 11.8, 4 = 13.4, 5 = 10.3, 6 = 9; (d) 1 = 15.4, 2 = 18.5, 3 = 13.5, 4 = 11.6, 5 = 12.4

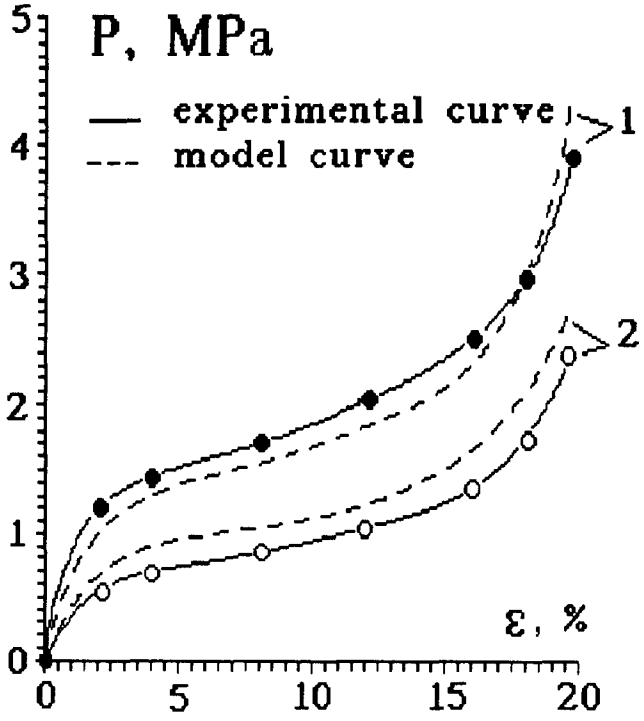

Fig. 3 Relationship between HIP forces and degree of consolidation. 1, Normal deformation; 2, SP deformation

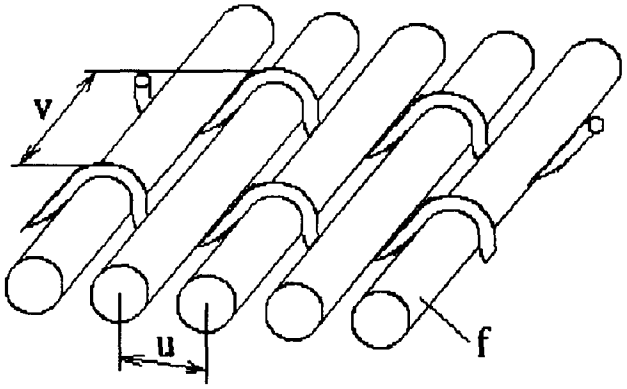

Fig. 4 Reinforcing net of boron fibers and metallic wire

Table 1 Characteristics of SP matrix aluminum foils

Alloying elements, %	d, μm	t_{sp}, °C	σ_{50}, MPa
6.4 Mg, 0.63Mn	6.3	475	6.5
1.1Si, 0.5Cu, 0.9Mg	7.8	490	8.4
6.5Cu, 0.6Mn, 0.4 Mg	18	475	15
5.99Cu, 0.39Zr	2.5	450	11
5.1Mg, 1.8Li, 0.12Zr	4.5	450	4.8

content that is required. The step is controlled by tuning of the loom and does not depend on wire diameter in some cases. The spacing between the wires, V, depends on wire and fiber diameters and fiber stacking step and is determined by a specific procedure. For example, when 0.05 mm diam aluminum wire is used for fixation of 0.14 mm diam boron fibers at a step of 0.17 mm, the optimal spacing, V, should be 4.8 mm.

Aluminum alloys in the form of a rolled foil were used as a matrix material. For most commercial alloys, a SP state is achieved by special preparation of their structure. This preparation consists of intense deformation and recrystallization annealing (Ref 13). It should be noted that the microstructure and deformation behavior of foils differ from those of thick specimens. The microstructure of foils is finer and stable whereas the superplasticity is less evident (Ref 16). If the foil width is less than ten grain sizes, superplasticity is not observed (Ref 20, 21). The main task is to choose the proper alloy and to determine the regimes of rolling and annealing in terms of a combination of structure preparation and achievement of the given thickness. For square fiber stacking, the foil thickness, t, can be expressed as:

$$t = \frac{U^2 - S_f}{U} = \frac{\frac{\pi D^2}{4V_f} - \frac{\pi D^2}{4}}{\frac{\sqrt{\pi D^2}}{4V_f}} = \frac{D\sqrt{\pi V_f}}{2}\left(\frac{1}{V_f} - 1\right) \quad \text{(Eq 5)}$$

Where U is fiber stacking step, S_f is an area of the fiber cross section, D is the fiber diameter, V_f is the volume fiber content in the compostite. For D = 142 μm and V_f = 0.5, as an example, the foil thickness is equal to 90 μm.

Equipment that allowed control of grain growth was used for rolling and annealing of foils (Ref 13). The characteristics of superlastic matrix foils are shown in Table 1. The parameters are defined in the following way: d is grain size, t_{sp} is temperature of superplasticity, and σ_{50} is true flow stress at 50% strain.

3.2 *Dimensioning and Cutting of Stocks*

The cutting of matrix foil and fiber nets into stocks of the required shape and size was performed by a computer controlled on a laser setup. This manipulation is particularly important for intricately shaped parts such as GTE blades.

A drawing of a part and a list of its mechanical properties are starting data for dimensioning. The reinforcement direction of each layer and the fiber volume fraction are determined depending on part shape and required properties. The fiber volume fraction in turn dictates a fiber stacking step, matrix foil thickness, and the shape and number of layers. The as-prepared stocks were assembled together in a packet, woven by a fine wire, and placed in a press form.

3.3 *Structure Investigation Techniques*

To reveal the deformation mechanisms acting during consolidation of fiber-reinforced composites and their effect on the fiber-matrix interface structure, the formation of a deformation relief on a surface of polished matrix foils was examined. For this purpose the packet of stocks was consolidated to different degrees; then the matrix plates were separated from the fibers and the surface of the matrix examined by scanning electron microscopy (SEM). The interface structure was stud-

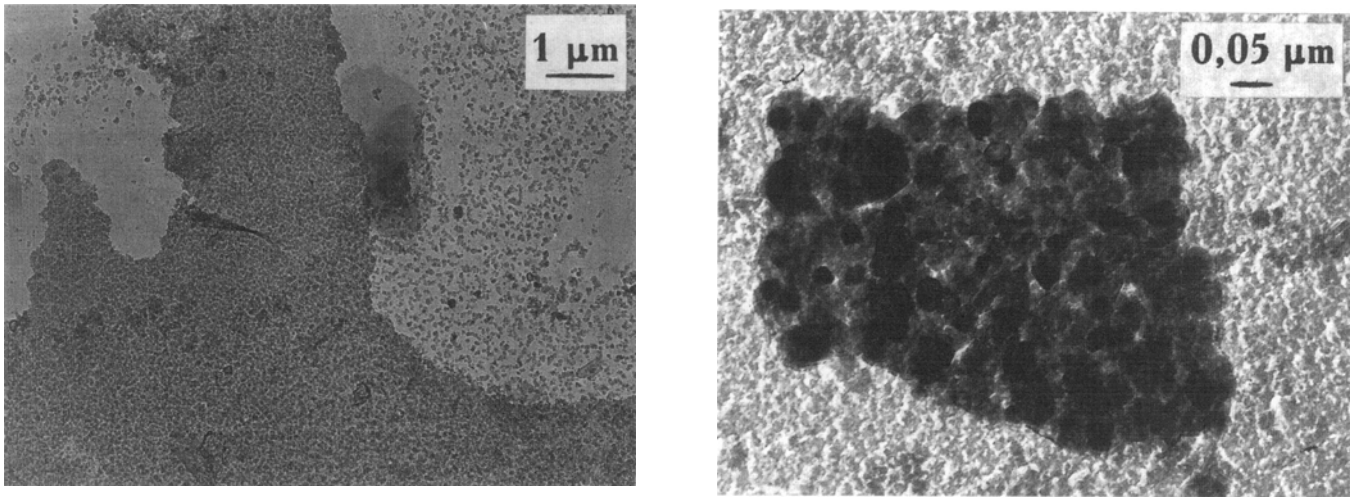

(a) (b)

Fig. 5 Reaction products at fiber-matrix interface. (a) Fine crystalline boron. (b) Dispersed aluminum borides

ied by means of extraction replicas from the surface of extracted fibers in a transmission electron microscope (TEM).

For nondestructive examination of parts, acoustic emission (AE) was used to characterize the interface. Composite samples containing eight layers of boron nets and nine layers of aluminum foil were used. Parameters for AE were measured by a standard acoustic device with a broad-band width piezoelectric transducer. Localized radiation heating with thermocycling was used to generate the AE signals. This caused the initiation of elastic stresses in specimens due to the difference in thermal expansion coefficients of fibers and matrix. Each thermo cycle was equal to 60 s (heating for 30 s and cooling for 30 s).

3.4 *Measurement of Interfacial Bond Strength*

Interface bond strength was measured by pulling a single fiber from the aluminum matrix (Ref 4). For this purpose aluminum plates were deformed between the fibers of one layer of the boron net by a special clamp that provided a small interaction area of the fiber with the matrix (approximately 1 mm of the fiber length). The samples were subjected to vacuum annealing for various time periods to obtain different degrees of component interaction. Finally, one after the other, fibers were pulled from the matrix, which was held in the pneumatic action grips of a standard Instron machine.

4. Results and Discussion

It has been shown that SP deformation affects solid-phase bonding (Ref 22-24). Consequently, matrix flow should be expected to affect the nucleation and growth of reaction products at the fiber-matrix interface during consolidation of fiber-reinforced composites under SP conditions.

A boron-aluminum composite was investigated. In previous papers (Ref 25, 26), the process of boron fiber/aluminum interface formation at early stages of their interaction was studied without considering the effect of matrix deformation processes. It has been shown that the boron fiber/aluminum interface reaction has two stages. In stage 1, dispersed aluminum borides are formed at the interface by these reactions:

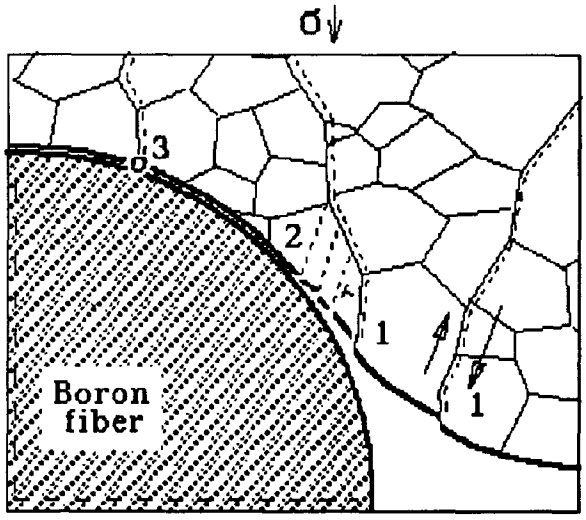

Fig. 6 Schematic of matrix deformation in the process of composite consolidation. See text for details.

$$B_2O_3 + 2Al = 2B + Al_2O_3 \quad \text{(Eq 6)}$$

$$nAl + mB = Al_nB_m \quad \text{(Eq 7)}$$

As Eq 6 shows, alumina and fine crystalline rhombohedral boron (Fig. 5a) are formed due to the aluminothermal reduction of the oxide film on the boron fiber. Then aluminum reacts with this fine-crystalline boron and dispersed aluminum borides are formed by Eq 7 (Fig. 5b). It is significant that these reactions do not affect fiber strength. In stage 2, borides are formed by direct reaction with the fibers, resulting in a notch on the fiber surface which can extend into the fibers and thus significantly reduce their strength.

The effect of matrix superplastic deformation on the fiber-matrix interface reaction then was investigated. Several important features must be considered. First, the plastic flow is nonuniform. As a rule, it localizes in the form of deformation bands (Ref 27-29). The nonhomogeneous flow can lead to a nonhomogeneous interaction at the fiber-matrix interface and a considerable decrease in composite strength.

Second, during composite consolidation the matrix material flows in thin clearances (about 20 μm) between strengthening fibers. Since a clearance width matches a grain size, the character of flow can differ considerably from that in thick specimens (Ref 21). It was established that in the process of fiber-reinforced composite fabrication the localization of matrix deformation takes place in the form of cooperative grain-boundary sliding (GBS) and intragranular sliding (IGS) (Ref 19). The localization results in characteristic oxide layer cracks on the matrix (Fig. 6). The formation of cooperative GBS bands is shown by the numerals 1 and 3, and the traces of IGS lines are indicated by the numeral 2 in Fig. 6.

The mechanism of matrix deformation determines a type of fiber-matrix interaction at the interface. Thus, after additional annealing at 520 °C for 6 h to cause a growth of the fiber-matrix reaction, the following was observed at the interface. The intensive interaction bands consisting of large boride crystals formed by a direct reaction with the fiber were observed in zones of intensive deformation with oxide layer cracks that developed along cooperative GBS steps (Fig. 7a). The interface reaction proceeded with the formation of the dispersed borides in zones with oxide layer cracks caused by the progression of IGS (Fig. 7b). Finally, in less intensive deformation zones where oxide layer cracks were not observed, the formation of spinel-type $n Al_2O_3 x B_2O_3$ occurred due to a direct contact of oxide films of aluminum with the boron fiber. The second and third types of these interactions do not affect fiber strength. It should be noted that the first type of interaction along cooperative GBS steps was observed after additional annealing and proceeded by the second type with formation of the dispersed borides at earlier stages of the interface reaction.

The measurement of fiber-matrix interface strength at different types of interactions shows that in the presence of mainly dispersed borides at the interface this strength is equal to 60 MPa, with a distribution variation coefficient of 6%. In the presence of predominantly spinel-type oxide bonds the strength is equal to 30 MPa, with a coefficient of 14%. Finally, in the case of the first type of interaction at the interface, the strength decreases to 48 MPa and the distribution variation co-

Table 2 Mechanical properties of the boron-aluminum composites: Boron fibers in three different matrices

Property	Matrix		
	Al-6.4Mg-0.63Mn	Al-6.5Cu-0.6Mn-0.4Mg	Al-1.2Si
Fiber strength, MPa	2500	2500	2500
Boron fibers, vol%	30	48	42
Density, g/cm^3	2.68	2.65	2.65
Tensile strength, MPa	1000	1300	1400
Transverse strength, MPa	180	200	230
Bending strength, MPa	...	2140	2160
Shear strength, MPa	...	160	145
Impact strength, MJ · m^{-2}	5.5	4.8	5.2
Tensile strength at 150 °C, MPa	860	1200	1100
Transverse strength at 150 °C, MPa	160	150	175

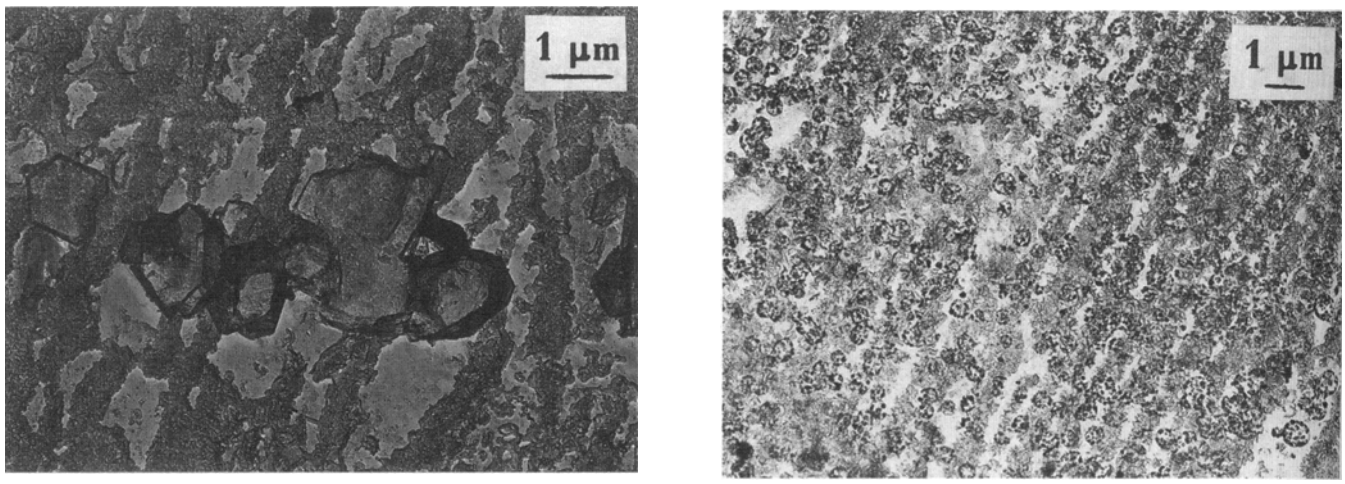

(a) (b)

Fig. 7 Interfacial reaction on extraction replicas. (a) In zones with oxide layer cracks that develop along cooperative GBS steps. (b) In zones with oxide layer cracks caused by progression of IGS

efficient rises to 43%. The experimental data showed that composite strength decreased in the case of the first type of interaction and achieved optimum values when the second and third types of interactions took place (Ref 30). Values of σ_c/σ_f^0 of boron-aluminum specimens in relation to composite annealing time are shown in Fig. 8, where σ_c is the composite strength and σ_f^0 is the original fiber strength.

Thus, three types of interactions can be distinguished in the composite: optimal, insufficient, and excessive. The optimal interaction consists of formation of a sufficient amount of dispersed borides and spinels at the interface. In this interaction, fibers do not degrade and maximum composite strength is achieved. In the insufficient interaction, the interface consists primarily of spinels. The excessive interaction is characterized by the presence of aluminum borides at the interface, which causes a loss of fiber strength and finally results in extraordinary reduction of mechanical properties (Ref 4).

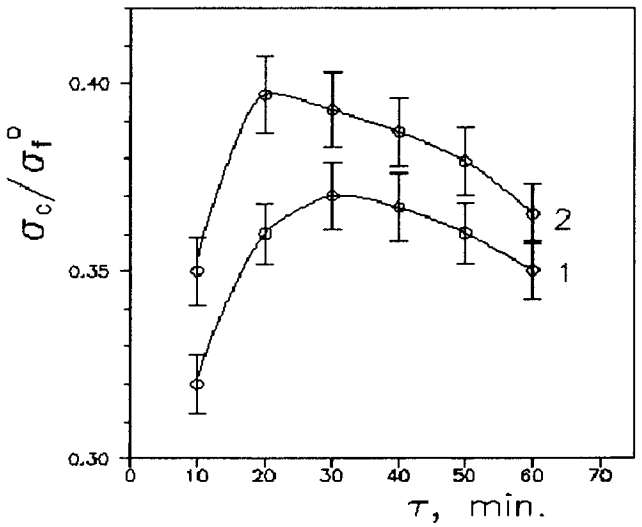

Fig. 8 Values of σ_c/σ_f^0 of a boron-aluminum composite for various annealing times under pressure for coarse (1) and fine-grain (2) matrices

The effect of matrix deformation on interface reaction and composite strength is still under investigation. Nevertheless, it is apparent that this effect is of great practical importance. In the case of full-scale production, nondestructive testing of the interface structure of finished products is necessary.

This study attempted to establish the relationship between different levels of interactions in the composite and characteristics of the AE method, which is known to be sensitive to structural defects (Ref 31). The energy distributions of AE signals in boron-aluminum samples with three different levels of interaction are presented in Fig. 9. These interactions initially were identified by the method of structural analysis. It can be seen that the AE signal spectra energy are considerably different in these states. For example, in samples with insufficient interaction (Fig. 9a), a small amount of low-energy signals were generated by the first heating; as the number of cycles increased, the amount and energy of these signals decreased. This is explained by the breaking of weak oxide bonds at interfaces and matrix-matrix connections. In samples with excessive interaction (Fig. 9b), a large number of high-energy AE signals were observed at the first cycle, and their intensity was three times higher than in the case of the insufficient interaction. This corresponds to failure of the fibers. The increase in the number and their energy of signals during further annealing confirmed this. By contrast, in samples with optimal interaction (Fig. 9c), signals were not observed up to the sixth cycle of thermoloading. Thus, the AE method combined with thermoloading allows levels of interaction in finished parts to be easily distinguished.

This complex approach has led to development of an MMC production technique that considerably increases mechanical properties (Table 2). Using this technique, composite GTE blades were manufactured (Fig. 10). They were subjected to full-scale testing and displayed good properties. The same approach was used to produce composite samples with titanium alloy or intermetallic matrices, confirming its versatility.

References

1. V.V. Vasilyev and V.D. Protasov, *Composite Materials,* Machine-Building, Moscow, 1990 (in Russian)

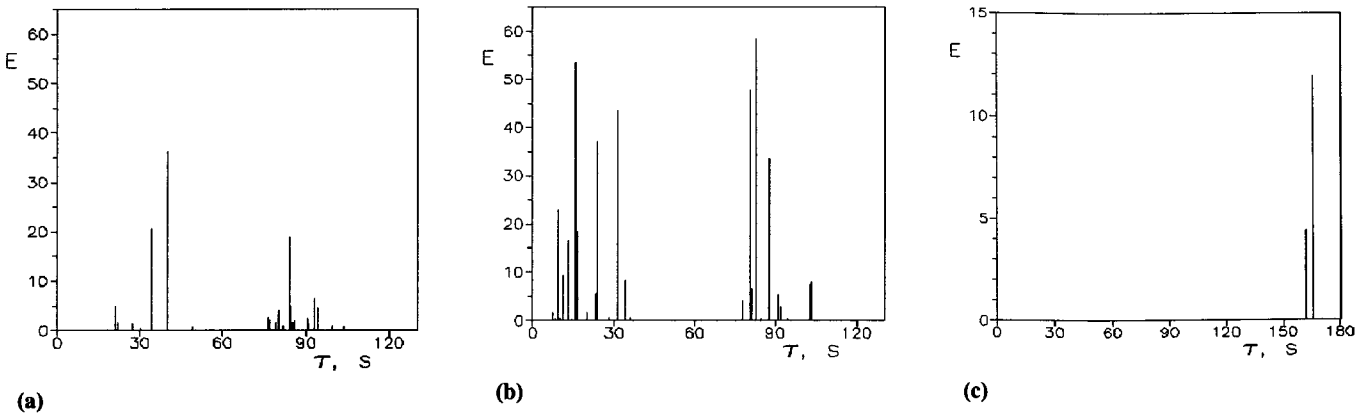

Fig. 9 Distribution of AE energy signals with time for boron-aluminum samples with different types of interactions at the fiber-matrix interface after HIP consolidation under a pressure of 30 MPa. (a) Insufficient interaction (2 min at 450 °C). (b) Excessive interaction (60 min at 510 °C). (c) Optimal interaction (10 min at 450 °C)

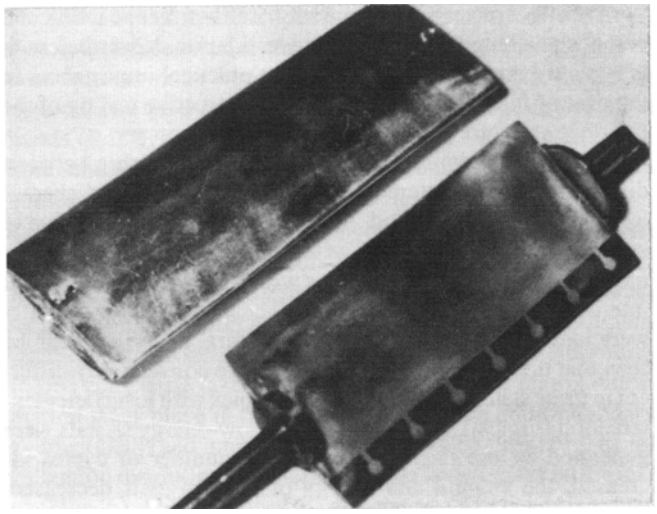

Fig. 10 Composite GTE blades. The large blade is 21 cm in length

2. M.H. Shorshorov, *Fiber-Reinforced Metal Matrix Composites,* Machine-Building, Moscow, 1981 (in Russian)
3. K.G. Kreider and K.M. Prevo, *Composite Materials,* World, Moscow, 1978 (in Russian)
4. A.G. Metcalfe, *Composite Materials,* World, Moscow, 1978 (in Russian)
5. Y. Uchiyama and M. Hasaka, Application of Superplasticity for Fabrication of Metal Matrix Composites, *Superplasticity in Advanced Materials,* S. Hori, M. Tokizane, and N. Furushiro, Ed., Japan Society for Research on Superplasticity, 1991, p 361-366
6. D.J. Lloyd, Fabrication of Fiber Composites Using an Aluminium Superplastic Alloy as Matrix, *J. Mater. Sci.,* Vol 19, 1984, p 2488-2492
7. M.H. Shorshorov and A.S. Tichonov, *Superplasticity of Metallic Materials,* Science, Moscow, 1973 (in Russian)
8. O.A. Kaibyshev, V.V. Astanin, and A.A. Sirenko, Peculiarities of the Structure and Properties of Superplasticity Produced B-Al Composites, *Int. Conf. Advanced Composite Materials,* T. Chandra and A.K. Dhingra, Ed., Minerals, Metals, and Materials Society, 1993, p 1147-1151
9. M.H. Shorshorov, Welding Titanium Alloys in Solid State under Superplastic Conditions, *Weld. Prod.,* Vol 10, 1975, p 20-22
10. P.J. Winkler, Diffusion Bonding and Superplastic Forming, Two Complementary Manufacturing Techniques, *Superplasticity and Superplastic Forming,* C.H. Hamilton and N.E. Paton, Ed., Minerals, Metals, and Materials Society, 1988, p 491-506
11. O.A. Kaibyshev, R.Ya. Lutfullin, and V.K. Berdin, The Effect of Superplasticity on the Solid State Weldability of the Titanium Alloy Ti-4.5Al-3Mo-1V, *Acta Metall.,* Vol 42 (No. 8), 1994, p 2609-2615
12. R.Ya. Lutfullin, R.M. Imayev, O.A. Kaibyshev, F. Hismatullin, and V.M. Imayev, Superplasticity and Solid State Bonding of the TiAl Intermetallic Compound with Micro- and Submicrocrystalline Structure, *Scr. Metall.,* Vol 33 (No. 9), 1995, p 1445-1449
13. O.A. Kaibyshev, *Superplasticity of Alloys, Intermetallides and Ceramics,* Springer Verlag, Berlin, 1992, p 254
14. R.L. Goetz, W.R. Kerr, and S.L. Semiatin, Modeling of the Consolidation of Continuous-Fiber Metal Matrix Composites via Foil-Fiber Techniques, *J. Mat. Eng. Perform.,* Vol 2 (No. 3), 1993, p 333-340
15. C.R. Ananth, N. Chandra, and H. Garmestani, Process Induced Residual Stresses in Metallic/Intermetallic Matrix Composites, *Computational Plasticity: Fundamentals and Applications,* D.R.J. Owen, E. Onate, and E. Hinton, Ed., Pineridge Press, 1992, p 2205-2216
16. V.V. Astanin, A.A. Sirenko, and V.N. Nikonov, The Effect of the Matrix Rheological Characteristics on the Consolidation of B-Al Composite, *Mech. Compos. Mater.,* Vol 5, 1988, p 878-883 (in Russian)
17. O. Zenkevich and K. Morgan, Finite Elements and Approximation, *Metallurgy,* Moscow, 1986 (in Russian)
18. A. Matusevith, Determination of Efforts of Composite Materials Strain, *Forge-Stamp Prod.,* Vol 12, 1981, p 24-28 (in Russian)
19. V.V. Astanin and L.A. Imayeva, The Effect of the Matrix Superplastic Deformation on Interface Reaction in Fiber-Reinforced Composites, *Scr. Metall.,* Vol 32 (No. 9), 1995, p 1495-1500
20. V.V. Astanin and A.A. Sirenko, Superplasticity of Foils of Al-5.8Mg-0.5Mn Alloy, *Metals,* Vol 4, 1990, p 132-136 (in Russian)
21. V.V. Astanin, Scale Factor and Superplasticity of Al-6% Cu-0.4%Zr Alloy, *Phys. Met. Metall.,* Vol 73 (No. 3), 1995, p 166-173 (in Russian)
22. V.V. Astanin and A.A. Sirenko, Structure, Properties and Destruction of Plasma-Sprayed Matrices for B-Al Composite, *Powder Metall.,* Vol 11, 1990, p 63-67 (in Russian)
23. O.A. Kaibyshev, R.Ya. Lutfullin, and V.K. Berdin, Nature of Diffusion Bonding Formation in State of Superplasticity, *Phys. Met. Metall.,* Vol 75 (No. 1), 1993, p 136-143 (in Russian)
24. Y. Maehara, Y. Komizo, and T.G. Langdon, Principles of Superplastic Diffusion Bonding, *Mater. Sci. Technol.,* Vol 4, 1988, p 669-674
25. V.V. Astanin and L.A. Imayeva, Early Stages of Boron Fiber/Aluminum Interface Formation, *Phys. Chem. Mater. Treat. (USSR),* Vol 4, 1993, p 128-135 (in Russian)
26. V.V. Astanin and L.A. Imayeva, Two Stages of Interfacial Reaction in B-Al Composite, *J. Mater. Sci.,* Vol 29, 1994, p 3351-3357
27. V.V. Astanin, O.A. Kaibyshev, and S.N. Faizova, Cooperative Grain Boundary Sliding under Superplastic Flow, *Scr. Metall.,* Vol 25 (No. 12), 1991, p 2663-2668
28. M.G. Zelin, N.A. Krasilnikov, R.Z. Valiev, M.W. Grabski, H.S. Yang, and A.K. Mukherjee, On the Microstructural Aspects of the Nonhomogeneity of Superplastic Deformation at the Level of Grain Groups, *Acta Metall. Mater.,* Vol 42 (No. 1), 1994, p 119-126
29. V.V. Astanin, O.A. Kaibyshev, and S.N. Faizova, The Role of Deformation Localization in Superplastic Flow, *Acta Metall. Mater.,* Vol 42 (No. 8), 1994, p 2617-2622
30. V.V. Astanin and A.A. Sirenko, Peculiarities of Formation of Interface Structure in B-Al Composites, *Int. Conf. Advanced Composite Materials,* MICC-90, Academy of Sciences of USSR, Moscow, 1990, p 115-116
31. E. Sokolova, N. Lutikov, and V. Thubuk, Sensitiveness of Acoustic Emission Parameters to Defects of B/Al Composite, *Mech. Compos. Mater.,* Vol 2, 1990, p 354-357